Proceedings of the 21st ICSMGE, Vienna, Austria, 14 – 19 June 2026. Pistrol, Adam & Schweiger (eds.)
Published by: ÖGG, Austrian Society for Geomechanics, Salzburg, Austria, ISBN 978-3-9503898-4-5
https://doi.org/10.53243/ICSMGE2026-631

Geological carbon dioxide injection efficiency considering SAG method at the pore scale

Seokgu Gang[1], Baek Seung Cheol[2], Jae-Eun Ryou[1], **Jongwon Jung[1]***
[1]Department of Civil Engineering, Chungbuk National University, Cheongju-si, South Korea, jjung@chungbuk.ac.kr
[2]Department of Civil Engineering, Gyeongkuk National University, Andong-si, South Korea

ABSTRACT: Deep aquifers are evaluated as promising structures for geological carbon storage in terms of storage capacity. Deep aquifers are a medium in which the pores are saturated with liquid, and capillary pressure acts during the injection of different fluids such as carbon dioxide. To solve this problem, the use of additives such as surfactants is considered. In this study, surfactant was used to reduce capillary pressure during carbon dioxide injection, and the effects of surfactant injection volume, and injection velocity (carbon dioxide) on injection efficiency were evaluated by applying a surfactant-alternating-gas injection method at the pore scale to consider the in-situ injection conditions. The results showed that carbon dioxide injection efficiency increased with increasing surfactant injection volume; Glucopon 600 CSUP exhibited a continuous rise to 0.87 PV, whereas SDBS reached a maximum near 0.44 PV and then slightly declined. The efficiency as a function of carbon dioxide injection velocity indicated pronounced improvement at 0.1 mL/min compared with 0.001 mL/min, and gains were limited under the lowest velocity regardless of surfactant type.

KEYWORDS: Aquifer, Geological storage, Carbon dioxide, Surfactant-alternating-gas, Micromodel.

1 INTRODUCTION

Geological carbon sequestration is reported as a promising method to solve global warming caused by carbon dioxide (CO_2). A deep aquifer is a storage layer structure for sequestration, and it is known to be promising due to its high storage capacity (Gale, 2004; Metz et al., 2005; Jones & Lawson, 2022). A deep aquifer is a porous structure saturated with fluids such as water inside. When using additives such as surfactants to improve the injection of CO_2 in a porous medium such as a deep aquifer, it is necessary to consider the conditions in which pore water exists.

The enhanced oil recovery (EOR) industry is applying the surfactant-alternating-gas (SAG) injection method, which injects CO_2 after pre-injecting surfactants into a storage layer where oil exists to increase the recovery rate of crude oil (Farajzadeh et al., 2009; Zhang & Agarwal, 2012; Sun et al., 2021). Therefore, this study applied the SAG injection method to evaluate the injection efficiency of CO_2 when using surfactants in a deep aquifer condition saturated with water. The experiment was performed under the condition that the pore water was pure water, and the injection efficiency was evaluated by first injecting the surfactant according to the concentration and injection amount and then according to the injection velocity of CO_2.

Surfactants, or surface-active agents, play a crucial role in reducing capillary pressure between immiscible fluids in porous media, such as deep aquifers. Capillary pressure is primarily influenced by interfacial tension (IFT) and contact angle (CA). Based on this principle, researchers have investigated the effects of surfactants on IFT and CA under various temperature and pressure conditions. Their findings indicate that the IFT of CO_2 decreases with increasing pressure and converges at approximately 12 MPa (Liang et al., 2017; Fabien et al., 2022). The CA ranges from approximately 16° to 48° under temperature conditions of 35–100°C and pressure conditions of 8–15 MPa (Jung & Wan, 2012; Saraji et al., 2013; Mutailipu et al., 2019). The use of surfactants results in an IFT ranging from 5.4 to 18.5 mN/m. In the case of surfonic POA 25R2, the CA under liquid carbon dioxide conditions is approximately 71.6°, which is at least 20° higher than when no surfactant is used (Kim & Santamarina, 2014).

As a method to consider the pore structure of the actual storage layer, a method of fabricating a poly-di-methyl-siloxane (PDMS) micromodel by utilizing the pore and pore neck information extracted from the micro X-ray computed tomography (CT) image of the drill core is widely applied (Karadimitriou et al., 2013; De et al., 2022; Mansouri-Boroujeni, 2022). PDMS is a type of silicone polymer that exhibits viscoelasticity and is suitable for use in a laboratory-scale environment due to its transparency, non-toxicity, and non-flammability (Murakami et al., 1998). In addition, fabricating a micromodel based on PDMS is economically advantageous compared to fabricating it using SiO_2-based quartz or glass, and it is easy to handle because it can be reused (Karadimitriou et al., 2013).

2 MATERIALS & METHODS

2.1 *CO_2 injection system using PDMS micromodel*

The fluids used to evaluate the injection efficiency of CO_2 are deionized water (DI water), surfactant solution, and gaseous CO_2. The surfactant solution was prepared 0.01 wt% using sodium dodecylbenzene sulfate (SDBS) and Glucopon 600 CSUP.

A micromodel is a porous medium that forms a network by forming pores and pore trees. In this study, a PDMS micromodel based on a drill core micro X-ray CT image is fabricated to simulate the pore structure of an actual reservoir. The fabrication process of a PDMS micromodel considering the pore structure of an actual reservoir largely consists of micro X-ray CT image acquisition, image processing, pore network extraction, and CAD-based drawing creation. First, this study uses an X-ray CT image of the Berea sandstone. After that, the CT image is converted into a black-and-white binarized image through thresholding after adjusting the brightness and contrast using Image J software. After that, Pnextract software is used to obtain network information on pores and pore trees from the binarized image (Ryou et al., 2025). A two-dimensional CAD drawing is created based on the acquired pore network information. Finally, a PDMS micromodel is fabricated based on the two-dimensional pore network drawing (Fig. 1).

The application procedure of the SAG injection method using the PDMS micromodel-based injection system is as follows (Fig. 2). 1) Deionized water is injected into the PDMS micromodel using the syringe mounted on Pump B. 2) The surfactant solution is injected into the tube connecting the PDMS micromodel and the three-way valve using the syringe mounted on Pump A according to the injection amount of the experimental conditions (Table. 1). 3) The 100 kPa gaseous CO_2 formed through the Isco pump is injected after reducing the pressure to 10 kPa using the back pressure regulator (Fig. 3). 4) The CO_2 injection was performed by injecting

approximately 2,300 µL, which is 50 times the pore volume (46 µL) of the PDMS micromodel, and then photographing the injection efficiency using a micro lens camera. The quantitative injection efficiency is calculated using Image J software. Table 1 presents experimental conditions, including surfactant type, concentration, injection volume, and injection velocities for both the surfactant and CO_2. These velocities were set based on the range observed at distances of 0.02–70 m from the injection well at a GCS site, which is 0.84–4,190 m/d (0.00005–0.23 mL/min) (Chang et al., 2020).

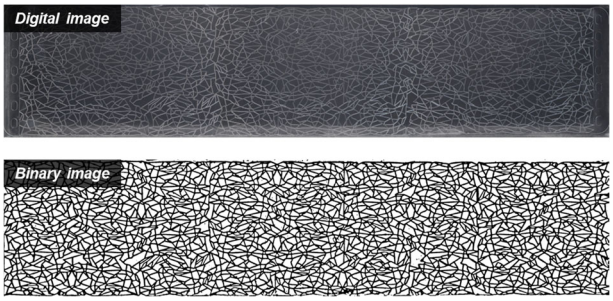

Figure 1. Digital and binary images of the fabricated PDMS micromodel.

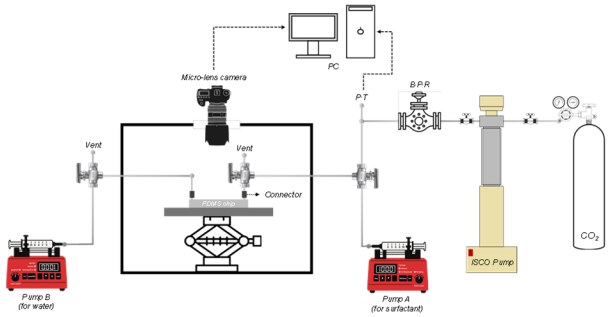

Figure 2. Schematic of CO_2 injection system using PDMS micromodel.

Table 1. Experimental condition for the SAG injection at the pore scale using surfactant

Case	1	2
Surfactant	SDS	Glucopon 600 CSUP
Concentration [wt%]	0.01	0.01
Surfactant injection volume [PV]		
Surfactant injection velocity [mL/min]	0.01	0.01
$scCO_2$ injection velocity [mL/min]	0.001, 0.01, 0.1	0.001, 0.01, 0.1

3 RESULTS AND CONCLUSION

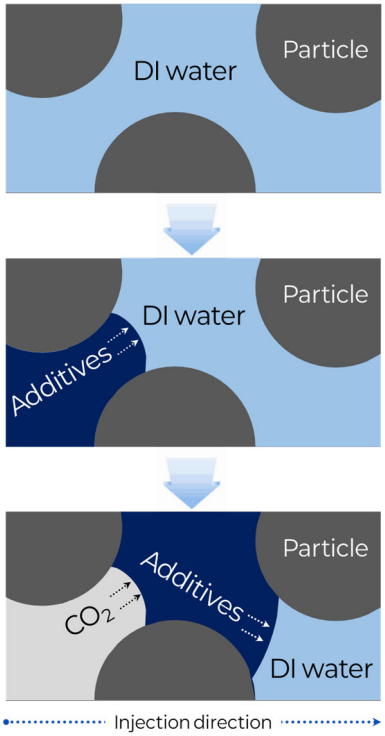

Figure 3. Procedure of the surfactant-alternating-gas injection at the pore scale.

3.1 *Effect of surfactant concentration*

Figure 4 shows the pore occupancy patterns according to the surfactant injection amounts (0.10, 0.22, 0.44, 0.87 PV; 5, 10, 20, 40 µL) when CO_2 was injected after pre-injecting the surfactant solution into the PDMS micromodel. The injection conditions are a constant velocity control of 0.01 mL/min for surfactants and 0.1 mL/min for CO_2. The red dotted box on the right in each image is a mark to emphasize the tendency of the CO_2-occupied area near the outlet to expand with increasing injection amount. At 0.10 PV, the fingering is prominent, leaving a large residual pore solution area, but as the injection amount increases, the continuity of the CO_2 stream improves, and the residual solution pockets decrease. Above 0.44 PV, the flow path becomes relatively stable, and at 0.87 PV, the CO2-occupied area continues to increase, but the velocity of increase becomes somewhat more gradual. These changes suggest that the surfactant solution injection amount contributes to controlling the movement path within the pores and reducing the residual phase, thereby improving the injection efficiency.

Figure 5 presents the pore occupancy pattern according to the surfactant injection amount (0.10, 0.22, 0.44, 0.87 PV; 5, 10, 20, 40 µL) when the PDMS micromodel was pre-injected with Glucopon 600 CSUP solution and then CO_2 was injected as a binarized image. The injection conditions are 0.01 mL/min of surfactant and 0.1 mL/min of CO_2. The red dotted box on the right side of each image is a mark to emphasize how the CO_2 occupied area expands near the outflow. As the injection amount increases, the area occupied by CO_2 in the area increases significantly, and the front continuity is also strengthened.

Compared to the previous results using SDBS, the following differences are observed. (1) At the same injection amount, the Glucopon condition reaches the outflow area faster or occupies a wider area, confirming the relative improvement in injection efficiency near the outflow. (2) At the initial

injection level (0.10–0.22 PV), SDBS showed more severe fingering and more residual aqueous phase pockets, whereas Glucopon showed a relatively homogeneous occupation pattern due to active micropore penetration. (3) Above 0.44 PV, the flow paths of both surfactants were stabilized, but in the case of Glucopon, even at the additional injection (0.87 PV), the residual aqueous phase around the outlet was further reduced, resulting in improved injection efficiency. This difference is interpreted as the result of the differences in the interfacial tension reduction characteristics and the intrapore movement mechanisms of the two surfactants directly affecting the injection efficiency and residual phase distribution.

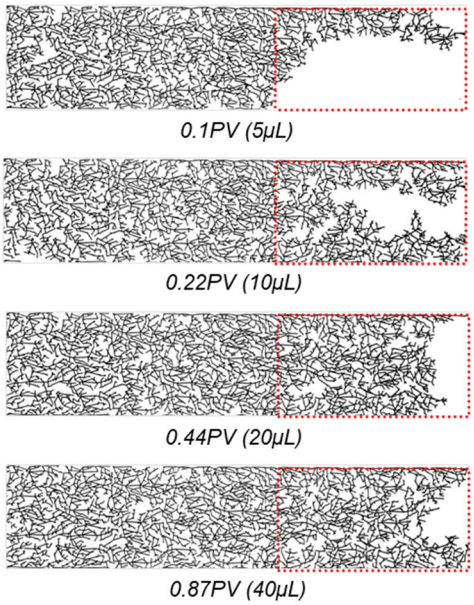

Figure 4. Binary images of the CO_2 injected PDMS micromodel with SDBS surfactant injection volume (surfactant injection velocity: 0.01 mL/min, CO_2 injection velocity: 0.1 mL/min).

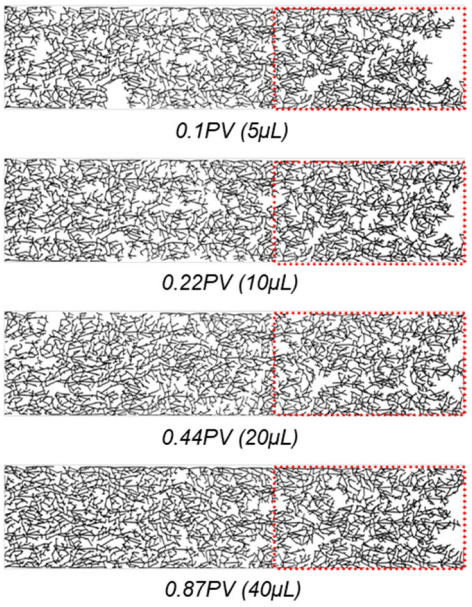

Figure 5. Binary images of the CO_2 injected PDMS micromodel with Glucopon 600 CSUP surfactant injection volume (surfactant injection velocity: 0.01 mL/min, CO_2 injection velocity: 0.1 mL/min).

3.2 *Effects of the surfactant injection volume*

Figure 6 compares the relationship between the surfactant injection volume (PV) and the CO_2 injection efficiency (%) under three CO_2 injection velocities (0.001, 0.01, and 0.1 mL/min). (a) shows the results for SDBS 0.01 wt%, and (b) shows the results for Glucopon 600 CSUP 0.01 wt%.

In the case of SDBS (Figure 6a), the injection efficiency rapidly increases to around 0.44 PV (around 90%) at 0.1 mL/min and then decreases slightly at 0.87 PV. At 0.01 mL/min, it increases to 0.44 PV and then converges (around 80%), and at 0.001 mL/min, only a gradual increase (around 60% → early 70%) is observed throughout the entire range. That is, SDBS has a large efficiency improvement with increasing injection amount at high CO_2 injection velocity, but there is a peak where the efficiency decreases after a certain injection amount.

In the case of Glucopon 600 CSUP (Figure 6b), the efficiency increases with increasing injection amount under all velocity conditions. At 0.1 mL/min, it continuously increases to 0.87 PV and reaches approximately 85% or more, and at 0.01 mL/min and 0.001 mL/min, it steadily increases to the mid-to-late 70% and around 70%, respectively. It is characterized by the fact that efficiency is maintained without a distinct peak.

When comparing the two surfactants, the efficiency difference is not large in the initial injection amount section (≤0.22 PV) at the same velocity, but SDBS shows a tendency to decrease after reaching the maximum efficiency at the intermediate injection amount during high-velocity injection, while Glucopon shows a stable increase throughout the entire section. This is interpreted because of the difference in the interfacial properties and pore distribution stability of the two surfactants being reflected in the injection efficiency behavior.

(a)

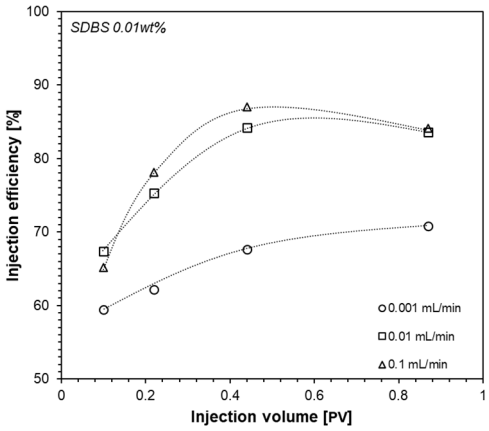

(b)

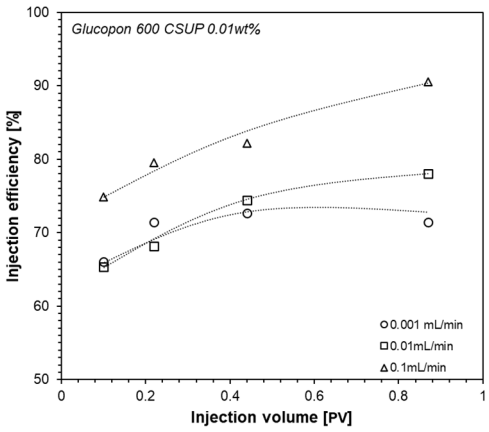

Figure 6. CO_2 injection efficiency with the surfactant injection volume (a) case of SDBS (b) case of Glucopon 600 CSUP.

4 CONCLUSIONS

This study compared and evaluated the injection efficiency change according to the injection amount (PV) and injection velocity by injecting CO_2 after pre-injection of surfactant in a PDMS micromodel. The binarized images were analyzed and the efficiency was evaluated under the same experimental conditions for SDBS (anionic) and Glucopon 600 CSUP (nonionic) 0.01 wt% solutions.

The binarized images showed that as the surfactant injection amount increased, the continuity of the CO_2 front improved, and the residual pore water decreased. In particular, the CO_2 occupied area gradually expanded near the outlet, suggesting that the increase in injection amount improved the efficiency around the outlet. Under the SDBS condition, fingering was significant at the initial injection amount, but under the Glucopon condition, relatively homogeneous injection was observed.

As a result of efficiency, the efficiency of SDBS increased rapidly to around 0.44 PV at high injection (0.1 mL/min) and then decreased slightly at 0.87 PV. On the other hand, Glucopon showed increased efficiency with increasing injection volume at all velocities, and the efficiency improvement effect was maintained even with additional injections. At low injection velocity (0.001 mL/min), the efficiency improvement was limited for both surfactants.

In the field, when using SDBS, a strategy is needed to avoid excessive injections by setting the optimal injection volume, and when using Glucopon, efficiency improvement can be expected over a relatively wide injection volume range. In addition, it was confirmed that controlling the CO_2 injection velocity was a key variable in improving efficiency. In future studies, scale-up verification considering high-salinity conditions, long-term residual behavior, and field-scale applicability is required.

5 ACKNOWLEDGEMENTS

This work was supported by 1) the Korea Institute of Energy Technology Evaluation and Planning (KETEP) grant funded by the Korean government (MOTIE) under project number 20212010200010, (2) National Research Foundation of Korea (NRF) grant funded by the Korean government (MSIT) under project number RS-2024-00353644.

6 REFERENCES

Chang C, Kneafsey TJ, Wan J, Tokunaga TK, Nakagawa S. Impacts of mixed- wettability on brine drainage and supercritical CO2 storage efficiency in a 2.5-D heterogeneous micromodel. Water Resour Res 2020;56(7). e2019WR026789.

De, N., Singh, N., Fulcrand, R., Méheust, Y., Meunier, P. and Nadal, F. (2022), Two-dimensional micromodels for studying the convective dissolution of carbon dioxide in 2D water-saturated porous media, Lab on a Chip, 22(23), 4645~4655.

Fabien, A., Lefebvre, G., Calvignac, B., Legout, P., Badens, E., & Crampon, C. (2022). Interfacial tension of ethanol, water, and their mixtures in high pressure carbon dioxide: Measurements and modeling. Journal of Colloid and Interface Science, 613, 847-856.

Farajzadeh, R., Andrianov, A., Bruining, H., & Zitha, P. L. (2009). Comparative study of CO2 and N2 foams in porous media at low and high pressure− temperatures. Industrial & Engineering Chemistry Research, 48(9), 4542-4552.

Gale, J. (2004). Geological storage of CO2: What do we know, where are the gaps and what more needs to be done. Energy, 29(9-10), 1329-1338.

Jones, A. C. Lawson, A. J. (2022). Carbon Capture and Sequestration (CCS) in the United States. Congressional Research Service.

Jung, J. W., & Wan, J. (2012). Supercritical CO2 and ionic strength effects on wettability of silica surfaces: Equilibrium contact angle measurements. Energy & Fuels, 26(9), 6053-6059.

Karadimitriou, N. K., Musterd, M., Kleingeld, P. J., Kreutzer, M. T., Hassanizadeh, S. M. and Joekar-Niasar, V. (2013), On the fabrication of PDMS micromodels by rapid prototyping, and their use in two-phase flow studies, Water Resources Research, 49(4), 2056~2067.

Kim, S., & Santamarina, J. C. (2014). Engineered CO2 injection: The use of surfactants for enhanced sweep efficiency. International Journal of Greenhouse Gas Control, 20, 324-332.

Liang, Y., Tsuji, S., Jia, J., Tsuji, T., & Matsuoka, T. (2017). Modeling CO2–water–mineral wettability and mineralization for carbon geosequestration. Accounts of chemical research, 50(7), 1530-1540.

Mansouri-Boroujeni, M. (2022), A microfluidic study of the physical and chemical mechanisms induced by CO2 injection in deep saline aquifers (Doctoral dissertation, Université d'Orléans).

Metz, B., Davidson, O., De Coninck, H. C., Loos, M., & Meyer, L. (2005). IPCC special report on carbon dioxide capture and storage. Cambridge: Cambridge University Press.

Murakami, T., Kuroda, S. I. and Osawa, Z. (1998), Dynamics of polymeric solid surfaces treated with oxygen plasma: Effect of aging media after plasma treatment, Journal of colloid and interface science, 202(1), 37~44.

Mutailipu, M., Liu, Y., Jiang, L., & Zhang, Y. (2019). Measurement and estimation of CO2–brine interfacial tension and rock wettability under CO2 sub-and super-critical conditions. Journal of colloid and interface science, 534, 605-617.

Ryou, J. E., Gang, S., Lee, J. Y. and Jung, J. (2025), Assessing surfactant influence on CO2 injection efficiency in geological storage: A pore network approach, Fuel, 381, 133598.

Saraji, S., Goual, L., Piri, M., & Plancher, H. (2013). Wettability of supercritical carbon dioxide/water/quartz systems: Simultaneous measurement of contact angle and interfacial tension at reservoir conditions. Langmuir, 29(23), 6856-6866.

Sun, X., Liu, J., Dai, X., Wang, X., Yapanto, L. M., & Zekiy, A. O. (2021). On the application of surfactant and water alternating gas (SAG/WAG) injection to improve oil recovery in tight reservoirs. Energy Reports, 7, 2452-2459.

Zhang, Z., & Agarwal, R. K. (2012). Numerical simulation and optimization of CO 2 sequestration in saline aquifers for vertical and horizontal well injection. Computational Geosciences, 16, 891-899.